

Glacier Ablation under Debris Cover: Field Observations on Lirung Glacier, Nepal Himalayas

BIRBAL RANA, MASAYOSHI NAKAWO, YUTAKA AGETA, AND KATSUMOTO SEKO
INSTITUTE FOR HYDROSPHERIC ATMOSPHERIC SCIENCES, NAGOYA UNIVERSITY

JUMPEI KUBOTA

TOKYO UNIVERSITY OF AGRICULTURE AND TECHNOLOGY

ATSUSHI KOJIMA

FACULTY OF AGRICULTURE, IWATE UNIVERSITY

Abstract

To evaluate glacier ablation under debris cover, a heavily debris-covered glacier in the ablation zone was observed. Ablation was measured at 30 places of different debris thickness, from clean ice to 13cm. The observations show that the ablation increased as debris thickness increased up to a certain thickness and then decreased as debris thickness increased further. The maximum ablation of 10cm/day was observed for the debris thickness of 2.6cm. Comparison of the observed ablation with the calculated value obtained from the energy balance equations shows that the calculated rate overestimates the observed rate. The calculated ablation rates are in good agreement when an increase in 1°C of surface temperature was assumed. The individual heat budget components show that radiation heat flux is the main energy source for glacier melt under the debris layer.

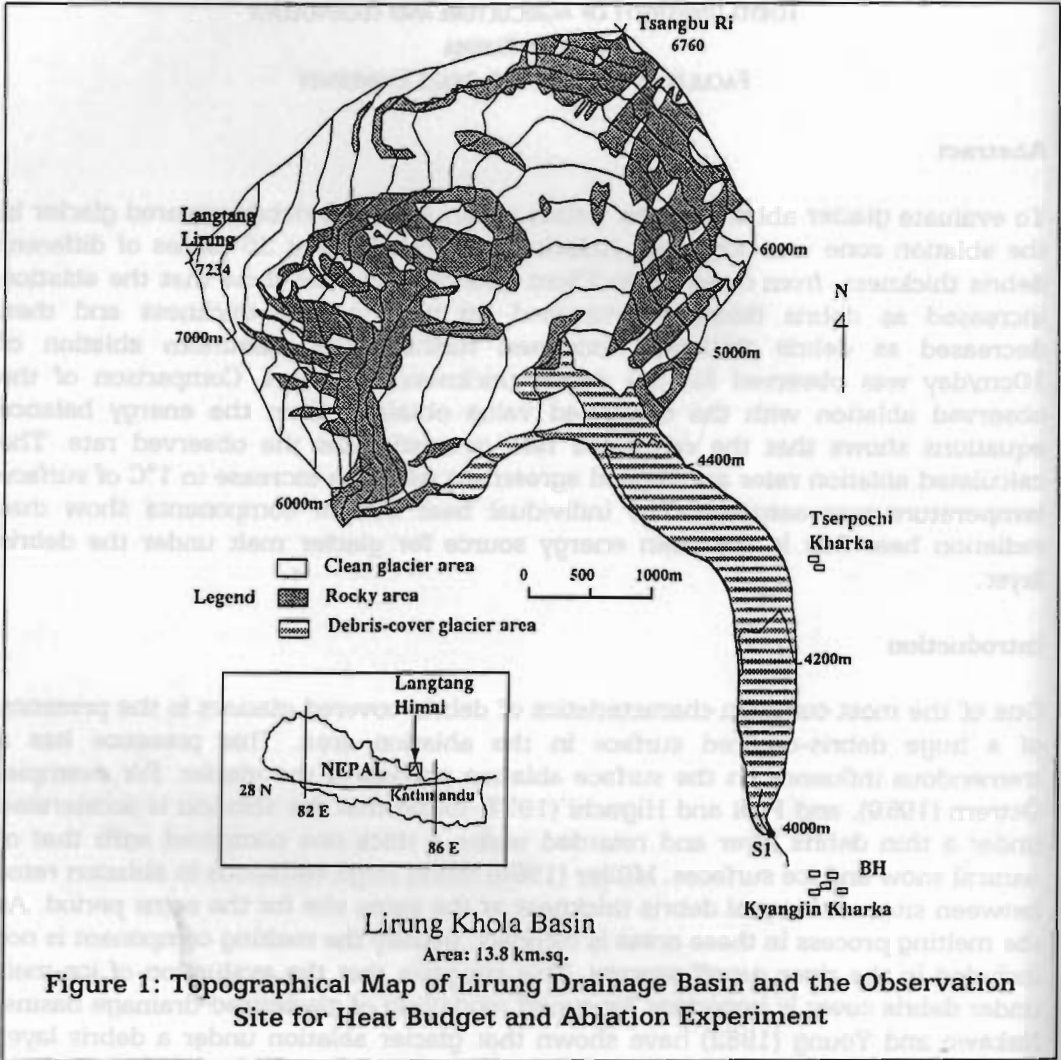
Introduction

One of the most common characteristics of debris-covered glaciers is the presence of a huge debris-covered surface in the ablation area. This presence has a tremendous influence on the surface ablation process of the glacier. For example, Östrem (1959), and Fujii and Higuchi (1977) found that the ablation is accelerated under a thin debris layer and retarded under a thick one compared with that of natural snow and ice surfaces. Müller (1968) found large variations in ablation rates between sites with equal debris thickness at the same site for the same period. As the melting process in these areas is complex, usually the melting component is not included in the river runoff process. This suggests that the evaluation of ice-melt under debris cover is important for runoff modelling of glacierised drainage basins. Nakawo and Young (1982) have shown that glacier ablation under a debris layer can be estimated from surface temperature and meteorological variables. In order to evaluate this melt, field observations were made from June 18 to 21, 1995, near the active terminus of Lirung Glacier, in the Nepal Himalayas. The purpose of this study was to evaluate the glacier ablation under debris cover using the heat budget equations and to test the contribution of each heat budget component.

Observation Site and Method of Data Collection

Since 1981, different types of glaciological, hydrological, meteorological, and geomorphological studies have been carried out in the Langtang Valley, 60km

north of Kathmandu, Nepal. Lirung Glacier, having a total drainage basin area of 13.8sq.km., 16 per cent of which is debris-covered, is located in this valley. The ablation zone is located in the southern direction, its lowest elevation being 4,120m — the lowest in this valley (Shiraiwa and Yamada 1991), which means large glacier melt from the ablation zone. Figure 1 shows the Lirung Glacier and the experimental site.



Heat budget observations at an altitude of about 4,350masl, including air temperature, relative humidity, wind speed, ground heat flux, and surface temperature, were recorded in a data logger every five minutes from June 17th to 21st. At a nearby site, ablation measurements were conducted at 30 places with different debris thickness, from a clean ice surface to 13cm-thick debris. The site was artificially prepared after clearing away the big boulders from the experimental plot. A string was tied tightly on two drilled poles (painted white) at each end of the plot, and the vertical distance from the string to the debris surface was measured at fixed points twice a day, the difference being taken as the ablation under debris

cover. The surface temperature was measured by infrared thermometer during the ablation measurements. The albedo of the debris layer was 0.11, and that of the clean ice was considered to be 0.4.

Meteorological Conditions

Results of meteorological observations are shown in Figure 2. From them it is clear that the observations were carried out during very humid conditions and at low wind speeds. Air temperature fluctuated from 4°C to 9°C. Figure 3 shows the surface temperature distribution for different debris thicknesses: it increases as the debris thickness increases.

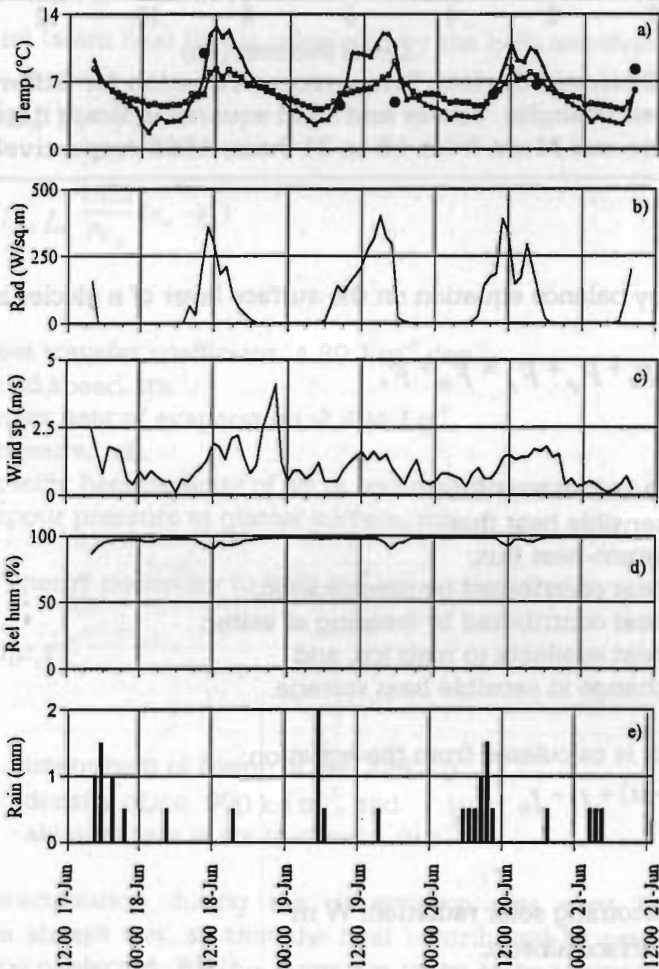


Figure 2: Meteorological Conditions at Lirung Glacier during Observation Period
 a) Air Temperature (square), Surface Temperature at Meteorological Station (triangle) and Surface Temperature for 13cm Debris Thickness (solid circles)
 b) Solar Radiation c) Wind Speed d) Relative Humidity e) Precipitation

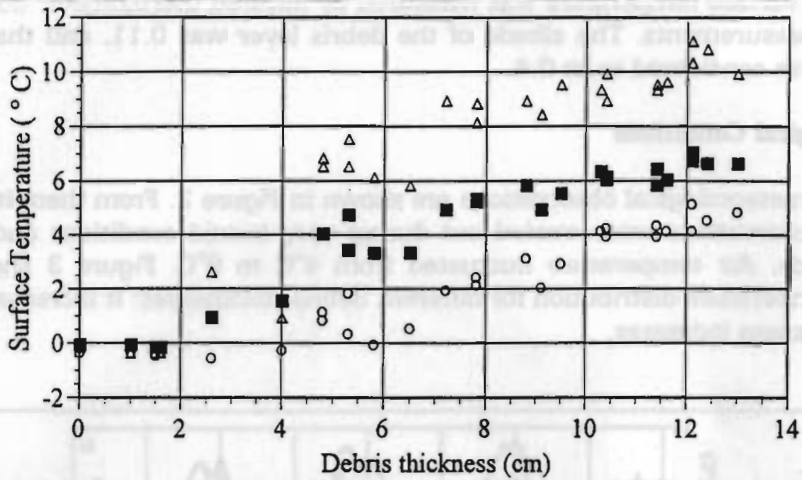


Figure 3: Observed Surface Temperature Variation for Different Debris Thickness (Open triangles, circles and solid squares indicate data for 18 and 19 June and Mean from 18 to 21 June, 1995 respectively.)

Model

The general energy balance equation on the surface layer of a glacier is given by:

$$F_r + F_h + F_l + F_p + F_f = F_m + F_s \quad (1)$$

where,

- F_r : radiation heat flux,
- F_h : sensible heat flux,
- F_l : latent-heat flux,
- F_p : heat contributed by precipitation,
- F_f : heat contributed by freezing of water,
- F_m : heat available to melt ice, and
- F_s : change in sensible heat storage.

Radiation heat flux is calculated from the equation:

$$F_r = Q(1 - \alpha) + I_i - I_o \quad (2)$$

where,

- Q : incoming solar radiation, $W m^{-2}$
- α : surface albedo,
- I_i : incoming long-wave radiation, $W m^{-2}$, and
- I_o : outgoing long wave radiation, $W m^{-2}$.

The incoming long-wave radiation can be calculated (Kondo 1967) by

$$I_i = \sigma(T_s + 273)^4 \{1 - (0.49 - 0.066\sqrt{e_s}) Cc\} \quad (3)$$

and the outgoing long-wave radiation by

$$I_o = \sigma (T_s + 273)^4 \quad (4)$$

where,

- σ : Stefan-Boltzmann constant, $5.67 \cdot 10^{-8} \text{ W m}^{-2} \text{ K}^{-4}$,
- T_a : air temperature, $^{\circ}\text{C}$,
- T_s : surface temperature, $^{\circ}\text{C}$,
- e_a : vapour pressure of air, mb, and
- C_c : depends on vapour pressure, cloud type, and cloud amount.

The sensible and latent heat flux is calculated by the bulk aerodynamic method

$$F_h = \beta U_a (T_a - T_s) \quad (5)$$

$$F_l = \beta U_a L_e \frac{0.622}{p C_p} (e_a - e_s) \quad (6)$$

where,

- β : heat transfer coefficient, $4.89 \text{ J m}^{-3} \text{ deg}^{-1}$,
- U_a : wind speed, ms^{-1} ,
- L_e : latent heat of evaporation, $2,494 \text{ J g}^{-1}$,
- p : pressure, mb,
- C_p : specific heat capacity of air at constant pressure, $1.0 \text{ J g}^{-1} \text{ deg}^{-1}$, and
- e_s : vapour pressure at glacier surface, mb.

The amount of energy necessary to melt the ice is calculated by

$$F_m = L_f \rho_i r \quad (7)$$

where,

- L_f : latent heat of fusion of ice, 334 J g^{-1} ,
- ρ_i : density of ice, 900 kg m^{-3} , and
- r : ablation rate in ice thickness, m s^{-1} .

The rate of precipitation during the observation was very low, and surface conditions were always wet, so that the heat contributed by precipitation and by freezing could be neglected. All the terms are taken to be positive downwards and are in W/m^2 . The assumptions made in the model are that the stored heat in the debris layer is constant and the temperature in the debris layer is in a stationary state. Thus, the final equation for estimating the surface ablation is given by:

$$F_r + F_h + F_l = F_m \quad (8)$$

Results

Observed ablation rates under different debris thicknesses are shown in Table 1. Figure 4a shows the observed ablation rate plotted against the debris thickness for daytime. It can be seen that the ablation increases as debris thickness increases up to a certain depth, and then decreases as debris thickness further increases. The maximum ablation of 10cm occurred for a debris thickness of 2.6cm in June. The debris thickness at which maximum ablation occurs is known as effective thickness. At sites with thinner debris than the effective thickness, the reflectivity of the surface ice is high, and thus less incoming energy is available for melting. At higher debris thickness, the energy is consumed in increasing the temperature of debris materials and only then conducted to melt the ice.

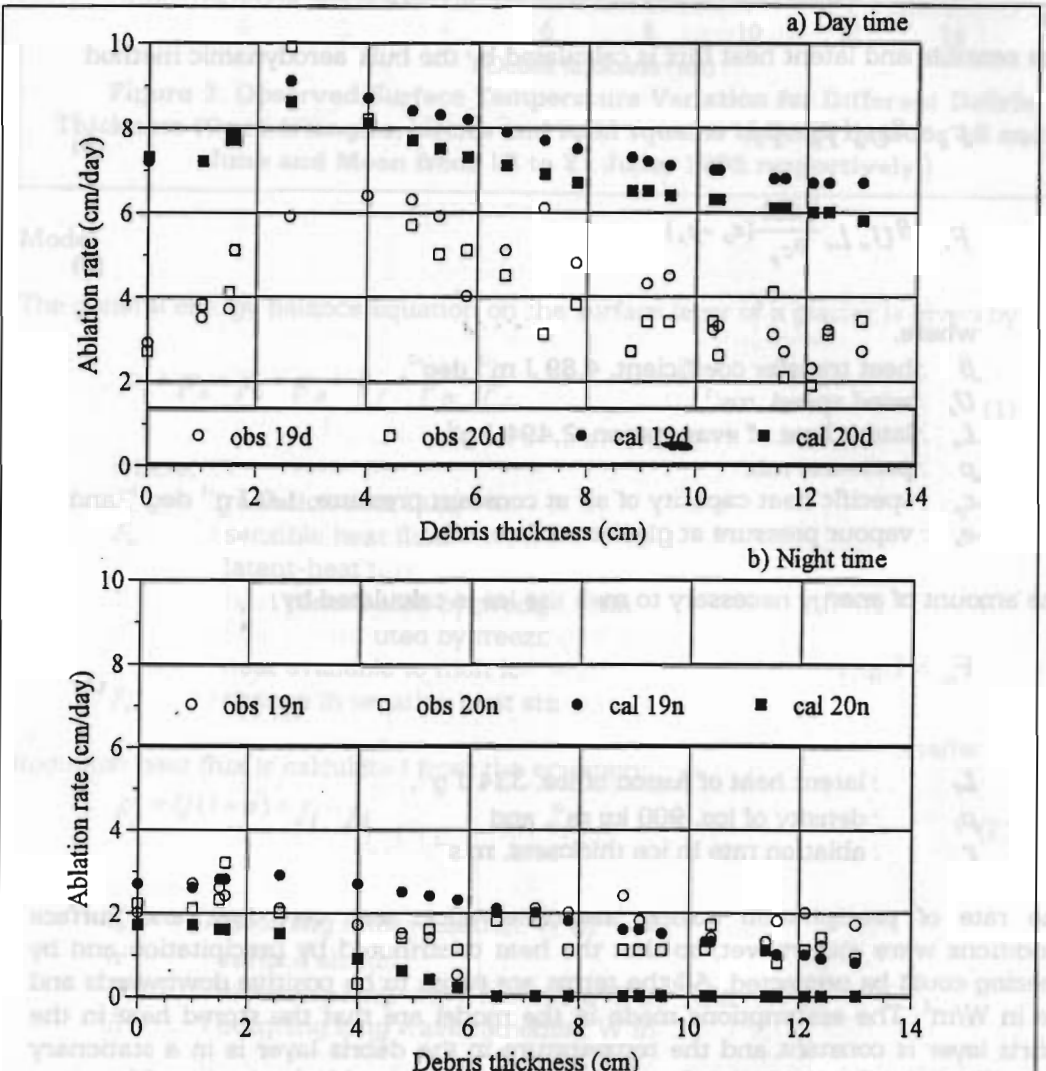


Figure 4: Comparison of Observed and Calculated Ablation (cm/day) (Open circles and squares indicates observed, solid circles and squares indicate calculated ablation for 19 and 20 June, respectively.)
 a) Day time and b) Night time

Table 1. Observed ablation data during 18-21 June 1995.

Debris thickness (cm)	Ablation (cm/day)					
	18-19	19-19	19-20	20-20	20-21	18-21
0	1.9	2.9	2.0	2.7	2.2	2.3
1.0	1.7	3.5	2.7	3.8	2.1	2.8
1.5	1.8	3.7	2.6	4.1	2.3	2.9
1.6	1.9	5.1	2.4	5.1	3.2	3.5
2.6	2.7	5.9	2.1	9.9	2.0	4.5
4.0	2.3	6.4	1.7	8.2	0.3	3.8
4.8	1.9	6.3	1.5	5.7	1.4	3.3
5.3	2.9	5.9	1.4	5.0	1.6	3.3
5.8	2.7	4.0	0.5	5.1	1.1	2.7
6.5	1.9	5.1	2.0	4.5	1.8	3.0
7.2	1.8	6.1	2.1	3.1	1.1	3.0
7.8	1.8	4.8	2.0	3.8	1.1	2.7
8.8	0.9	2.7	2.4	2.7	1.1	2.0
9.1	1.1	4.3	1.8	3.4	1.1	2.3
9.5	1.1	4.5	1.5	3.4	1.1	2.3
10.3	1.0	3.2	1.1	3.4	1.1	2.0
10.4	1.0	3.3	1.4	2.6	1.7	2.0
11.4	0.6	3.2	1.3	4.1	1.1	2.1
11.6	0.6	2.7	1.8	2.1	0.8	1.6
12.1	0.6	2.3	2.0	1.9	1.1	1.6
12.4	0.5	3.2	1.2	3.1	1.4	1.9
13.0	0.8	2.7	1.7	3.4	0.9	1.9

Figure 4b shows the observed ablation during the night. The observed ablation rate is almost constant for all debris thicknesses. The mean ablation rate during the whole observation period is shown in Figure 4c. The maximum mean ablation of 4.5cm/day occurred at a debris thickness of about 2.6cm. The debris thickness at which the ablation rate is the same as for clean ice is known as the critical thickness and is around 9cm.

The main object of the present heat budget study is to determine the relative importance of different terms of the heat budget components. The heat budget components for different debris thicknesses are shown in Figures 5a and 5b. The radiation heat flux increases as debris thickness increases up to a certain thickness and then decreases, but the percentage of energy contributed by it to melting the ice under it goes on increasing. This is mainly because the contribution of radiation heat flux increases as debris thickness increases due to a 30 per cent difference in the albedo. The sensible and latent heat flux components decrease as debris thickness increases and tend to be negligible for thicker debris layers during the night (Fig 5a), while during the day (Fig. 5b) they are the energy sink source. This means that radiation heat flux is the main energy source for ice-melt under the debris layer. Figure 6 shows that the contribution of long-wave radiation to ice-melt under the debris layer decreases as debris thickness increases, the surface radiating the energy back into the atmosphere.

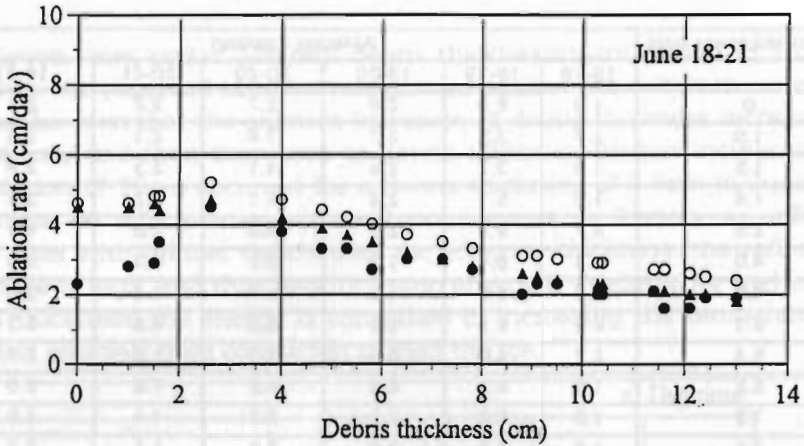


Figure 4c: Comparison of Mean Observed Ablation (solid circles) to Mean Calculated Ablation (open circles) during the Period from June 18-21 (Solid triangles indicates calculated ablation when surface temperature is increased by 1°C.)

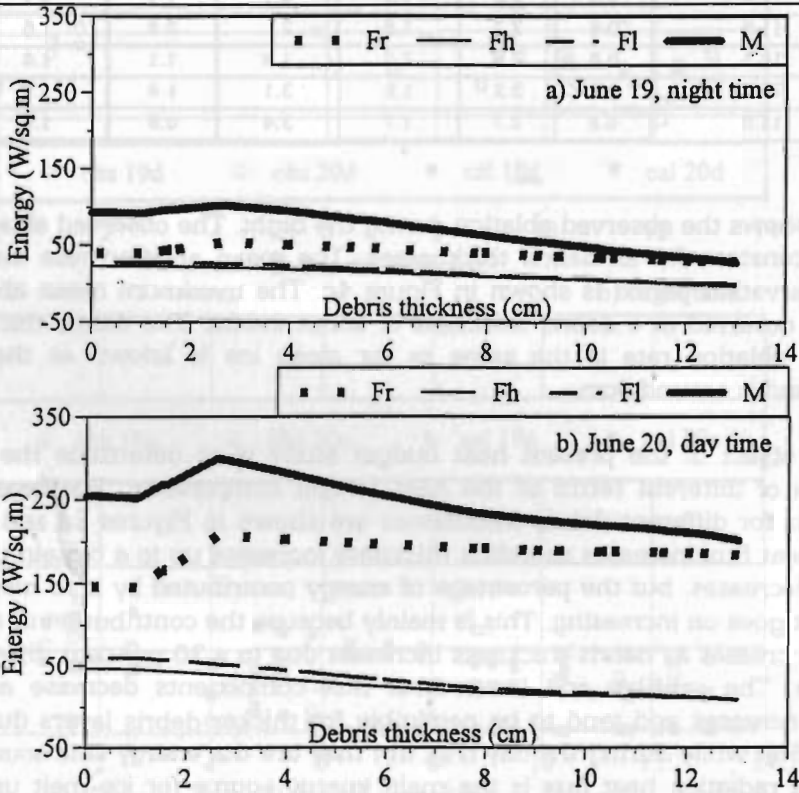
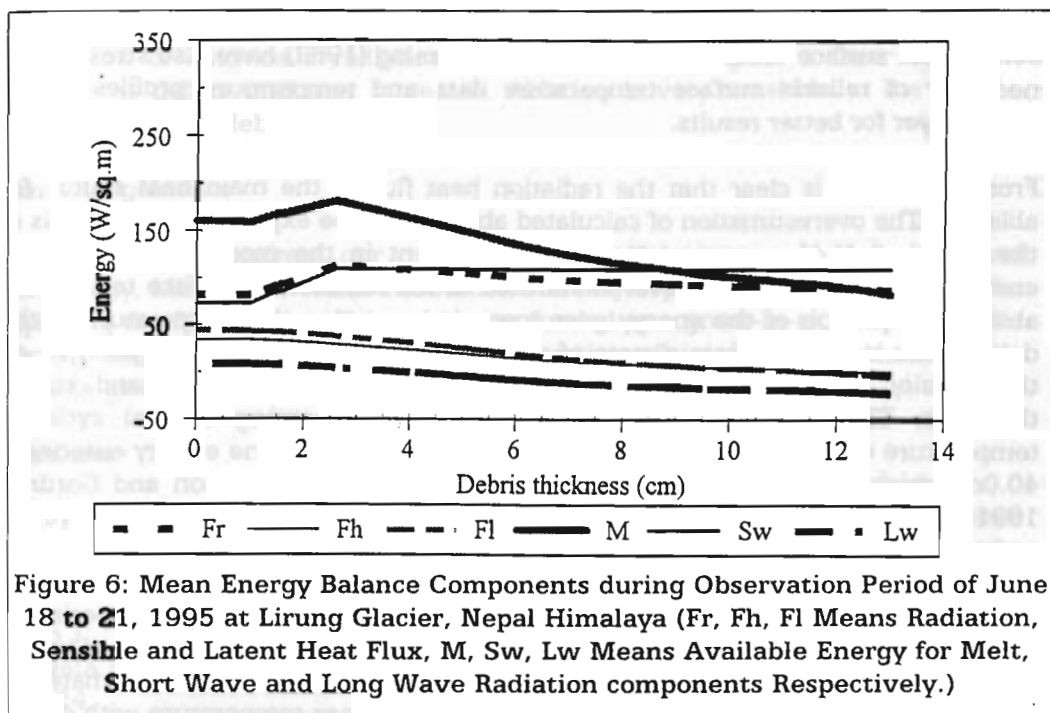


Figure 5: Comparison of Head Budget Components (Fr, Fh, Fl Indicates Radiation, Sensible and Latent Heat Flux, Respectively and, M, Indicates Energy Available for Melt.)

a) June 19, Night Time

b) June 20, Day time



Discussion

Comparison of the Ablation Results

From Figure 4a, we see that on both days, during the day, the calculated ablation rates are overestimated for all debris thicknesses. During the night (Fig. 4b), the results are comparable for both periods. The mean surface temperature for all debris thicknesses was underestimated, as the surface temperature was measured only twice a day. The variation in surface temperature during the day is significantly larger (Fig. 2a) than at night, which leads to greater differences in ablation during daytime. An increase in surface temperature means an increase in outgoing long-wave radiation and a decrease in radiation heat flux, sensible heat flux, and latent heat flux (equations 4, 2, 5, and 6), and so less energy is available for melt. The maximum ablation of 10cm/day was observed for June 20 at a 2.6cm debris thickness, while on the 19th the maximum ablation of 6.4cm/day occurred at a depth of 4cm. In a similar way, the critical thickness also differed from day to day, depending on total available energy for melting. The mean incoming solar radiation on the 19th exceeds that on the 20th. There is a significant difference in mean seasonal ablation rates between sites of varying debris thickness and also high variations in ablation rates at the same site over time (Mattson et al. 1989).

Sensitivity of Surface Temperature

The ablation rate was calculated for a debris surface temperature increased by 1°C to minimise the error in surface temperature. From Figure 4c it can be seen that the calculated ablation rate shows good agreement with the observed values when

the ablation rate is calculated in this way. This indicates that ablation is very sensitive to surface temperature. Nakawo and Young (1982) have also stressed the necessity of reliable surface temperature data and temperature profiles in the debris layer for better results.

From Table 2 it is clear that the radiation heat flux is the main heat source for ablation. The overestimation of calculated ablation can be explained on the basis of the assumption of constant heat storage inherent in the model. Not all of the energy entering the debris cover is shuttled to the ice/debris interface to promote ablation. A portion of the energy goes towards increasing the temperature of the debris; that is, it is put into a state of storage. The stored energy is dependent on the density, thermal diffusibility, and specific heat of the debris and on its thickness. The surface temperature data indicate a strong diurnal cycle of temperature change at the surface. More than 80 per cent of the energy entering a 40.0cm-thick debris cover on a sunny day can be stored (Mattson and Gardner 1991). This suggests that the evaluation of heat storage in the debris cover is necessary and should be included in the energy balance model studies. The above results are based on the results carried out under cloudy and humid conditions. To estimate the mean summer ablation, it will be necessary to conduct the experiment during clear weather conditions. The observations for the full ablation period would help to understand the ablation process under the debris cover and to estimate the exact ablation. Figure 3 illustrates the variation of surface temperature with debris thicknesses of up to 13cm only. From the ground-truth observations, the relation of surface temperature to debris thickness can be defined for much thicker debris layers also. Once this is done, using remote-sensing data (thermal band) or airborne observations (thermal imager), one can deduce the distribution of surface temperatures within the glacier basin, at which point the ablation from the debris-covered area of the glacier can be estimated and incorporated into the runoff modelling of river basins.

Table 2. Total energy fluxes (W/m^2) used for ablation at 2.6 and 13.0 cm debris thickness, h (cm)

Date	Jun 18-19		Jun 19-19		Jun 19-20		Jun 20-20		Jun 20-21		Jun 18-21	
	h, cm	2.6	13.0	2.6	13.0	2.6	13.0	2.6	13.0	2.6	13.0	2.6
F_r	45	100	70	87	53	100	69	92	39	sink	63	100
$F_{h,r}$	24	sink	13	6	21	1	13	4	26	sink	16	sink
$F_{l,r}$	31	sink	17	7	26	sink	18	4	35	sink	21	sink

Conclusions

The data indicate that the addition of debris to a clean ice surface initially increases the ablation rate, but then decreases it after reaching the critical debris thickness. This result shows the influence of debris cover thickness on ablation rates. The critical thickness and effective ablation varied from day to day. The maximum ablation of 10cm/day and the mean ablation of 4.5cm/day occur at 2.6cm of debris thickness. The radiation heat flux is the dominant energy source for glacier ablation. The contribution of convective heat fluxes to glacier ablation decreases as debris thickness increases. That influence of radiation heat flux increases as debris thickness increases is mainly due to the 30 per cent difference in albedo. The

surface temperature of the debris layer increases as debris thickness increases. The contribution of long-wave radiation to glacier ablation under a layer of debris decreases as debris thickness increases. Ablation is very sensitive to the surface temperature of the debris cover.

Acknowledgements

We would like to express our gratitude to the Department of Hydrology and Meteorology, Ministry of Water Resources, His Majesty's Government of Nepal, for supporting the filed survey. This study was funded as a grant-in-aid (060 4105) for scientific research by the Ministry of Education, Science and Culture of the Japanese government.

References

- Fujii, Y. and Higuchi, K., 1977. 'Statistical Analyses of the Forms of the Glaciers in Khumbu Region'. In *Journal of Japanese Society of Snow and Ice (Seppyo)*, 39, Special issue, 7-14.
- Kondo J., 1967. 'Analysis of Solar Radiation and Downward Long-wave Radiation Data in Japan'. *Scientific Report of Tohoku University*, ser. 5, 18, No 3, 91-124.
- Mattson, L.E. and Gardner, J.S., 1989. 'Energy Exchanges and Ablation Rates on the Debris-covered Rakhiot Glacier, Pakistan'. In *Zeitschrift fur Gletscherkunde und Glazialgeologie*, 25 (1), 17-32.
- Moribayashi, and Higuchi, K., 1977. 'Characteristics of the Glaciers in the Nepal Himalayas'. In *Journal of Japanese Society of Snow and Ice (Seppyo)*, 39, Special issue, 3-6.
- Müller, F., 1968. 'Mittelfristige Schwankungen der Oberflächengeschwindigkeit des Khumbu-Gletschers am Mnt. Everest'. In *Schweizerische Bauzeitung*, 86, 1-4.
- Nakawo, M. and Young, G.J., 1982. 'Estimate of Glacier Ablation under a Debris Layer from Surface Temperature and Meteorological Variables'. In *Journal of Glaciology*, 28, (98), 29-34.
- Östrem, G., 1959. 'Ice-melting under a Thin Layer of Moraine and the Existence of Ice Cores in Moraine Ridges'. In *Geogr. Ann.*, 41, 686-694.
- Shiraiwa, T. and Yamada, T., 1991. 'Glacier Inventory of the Langtang Valley, Nepal Himalayas'. In *Low Temperature Science, Series A*. No. 50. Data Report.